

UNCLASSIFIED

AD NUMBER

AD408626

NEW LIMITATION CHANGE

TO

**Approved for public release, distribution
unlimited**

FROM

**Distribution authorized to U.S. Gov't.
agencies and their contractors;
Administrative/Operational Use; 23 MAR
1963. Other requests shall be referred to
Army Electronics Research and Development
Lab., Fort Monmouth, NJ.**

AUTHORITY

ASClA ltr, 1 Mar 1965

THIS PAGE IS UNCLASSIFIED

AD-408626

Date: April 23, 1963

Project No. 302410

Copy No. 37

**FERROELECTRIC CERAMIC FILTERS,
IF TRANSFORMERS, AND NETWORKS**

Report No. 26

**Fifth Quarterly Report
1 December 1962 through 28 February 1963**

**Contract No. DA 36-039 SC-87275
DA Task No. 3A99-15-005-05**

**U. S. Army Electronics Research and Development Laboratory
Fort Monmouth, New Jersey**

Signal Corps Technical Requirement Number SCL-7534

The object of this contract is the development of piezoelectric
ceramic filters and devices at frequencies above 1 Mc.

By: D. R. Curran

D. J. Koneval

Approved: Hans Jaffe

Hans Jaffe, Director
Electronic Research

**Clevite Corporation
Electronic Research Division
Cleveland, Ohio**

ASTIA AVAILABILITY NOTICE

"Qualified requestors may obtain copies of this report from ASTIA. ASTIA release to OTS not authorized."

<p>AD Accession No. Clevite Corporation, Electronic Research Division, Cleveland, Ohio PATHELECTRIC CERAMIC FILTERS, IF TRANSFORMERS, AND NETWORKS Report No. 18 D. R. Carroll and D. J. Koval Fifth Quarterly Report, 1 December 1962 through 28 February 1963 Contract No. DA-36-039 SC-87275 DA Task No. 3499-15-005-03 Unclassified Report</p> <p>Application of existing theory for the propagation of elastic waves in thin plates appears to give a plausible explanation for the behavior of high frequency AT-cut quartz resonators and disk resonators on flat wafers. Experimental measurements of inter-resonator coupling and interaction between resonator and wafer edge appear to be in agreement with theory.</p> <p>Parallel combinations of quartz and ceramic resonators yield a strong zero and pole of impedance corresponding to resonance and antiresonance of the ceramic. A strong zero of impedance corresponds to resonance and antiresonance of the quartz, and a very weak pole contributed by the antiresonance of the quartz. The addition of parallel quartz resonators with appropriately located frequencies to a ceramic ladder filter should yield stable poles of attenuation defining the edge of the pass band without otherwise affecting the pass band behavior. Thickened expander resonators made of hot-pressed ceramic have substantially improved resonance response characteristics at 12 Mc over those using conventionally fabricated ceramic.</p>	<p>AD Accession No. Clevite Corporation, Electronic Research Division, Cleveland, Ohio PATHELECTRIC CERAMIC FILTERS, IF TRANSFORMERS, AND NETWORKS Report No. 18 D. R. Carroll and D. J. Koval Fifth Quarterly Report, 1 December 1962 through 28 February 1963 Contract No. DA-36-039 SC-87275 DA Task No. 3499-15-005-03 Unclassified Report</p> <p>Application of existing theory for the propagation of elastic waves in thin plates appears to give a plausible explanation for the behavior of high frequency AT-cut quartz resonators and disk resonators on flat wafers. Experimental measurements of inter-resonator coupling and interaction between resonator and wafer edge appear to be in agreement with theory.</p>
<p>AD Accession No. Clevite Corporation, Electronic Research Division, Cleveland, Ohio PATHELECTRIC CERAMIC FILTERS, IF TRANSFORMERS, AND NETWORKS Report No. 18 D. R. Carroll and D. J. Koval Fifth Quarterly Report, 1 December 1962 through 28 February 1963 Contract No. DA-36-039 SC-87275 DA Task No. 3499-15-005-03 Unclassified Report</p> <p>Application of existing theory for the propagation of elastic waves in thin plates appears to give a plausible explanation for the behavior of high frequency AT-cut quartz resonators and disk resonators on flat wafers. Experimental measurements of inter-resonator coupling and interaction between resonator and wafer edge appear to be in agreement with theory.</p> <p>Parallel combinations of quartz and ceramic resonators yield a strong zero and pole of impedance corresponding to resonance and antiresonance of the ceramic. A strong zero of impedance corresponds to resonance and antiresonance of the quartz, and a very weak pole contributed by the antiresonance of the quartz. The addition of parallel quartz resonators with appropriately located frequencies to a ceramic ladder filter should yield stable poles of attenuation defining the edge of the pass band without otherwise affecting the pass band behavior. Thickened expander resonators made of hot-pressed ceramic have substantially improved resonance response characteristics at 12 Mc over those using conventionally fabricated ceramic.</p>	<p>AD Accession No. Clevite Corporation, Electronic Research Division, Cleveland, Ohio PATHELECTRIC CERAMIC FILTERS, IF TRANSFORMERS, AND NETWORKS Report No. 18 D. R. Carroll and D. J. Koval Fifth Quarterly Report, 1 December 1962 through 28 February 1963 Contract No. DA-36-039 SC-87275 DA Task No. 3499-15-005-03 Unclassified Report</p> <p>Application of existing theory for the propagation of elastic waves in thin plates appears to give a plausible explanation for the behavior of high frequency AT-cut quartz resonators and disk resonators on flat wafers. Experimental measurements of inter-resonator coupling and interaction between resonator and wafer edge appear to be in agreement with theory.</p>
<p>AD Accession No. Clevite Corporation, Electronic Research Division, Cleveland, Ohio PATHELECTRIC CERAMIC FILTERS, IF TRANSFORMERS, AND NETWORKS Report No. 18 D. R. Carroll and D. J. Koval Fifth Quarterly Report, 1 December 1962 through 28 February 1963 Contract No. DA-36-039 SC-87275 DA Task No. 3499-15-005-03 Unclassified Report</p> <p>Application of existing theory for the propagation of elastic waves in thin plates appears to give a plausible explanation for the behavior of high frequency AT-cut quartz resonators and disk resonators on flat wafers. Experimental measurements of inter-resonator coupling and interaction between resonator and wafer edge appear to be in agreement with theory.</p>	<p>UNCLASSIFIED</p>

TABLE OF CONTENTS

	<u>Page</u>
Purpose	ii
Abstract	iii
Conferences	iv
Reports	iv
List of Illustrations	v
<u>Section</u>	<u>Title</u>
1. Factual Data	1
1. 1 AT-Cut Quartz Resonators	1
1. 2 Experimental Evaluation of Range of Action for Quartz Dot-Resonators	5
1. 3 Higher Frequency Quartz Resonators and Filters	9
1. 4 Combinations of Quartz and Ceramic Resonators	9
1. 5 Ceramic Resonators	10
2. Conclusions	11
3. Plans for Next Interval	12
4. Identification of Key Technical Personnel	13
5. Initial Distribution	14

PURPOSE

To perform research and development leading to the design of improved ferroelectric ceramic filters, IF transformers, and networks in the frequency range above 1 Mc. These should include two dimensional filters and networks with a multiplicity of resonators or network elements on a single wafer. Objectives are reliability, miniaturization, and improved performance characteristics over conventional filters in this range.

To fabricate samples illustrating the level of development achieved during this contract and the range of characteristics available as a result of this contract.

ABSTRACT

Application of existing theory for the propagation of elastic waves in thin plates appears to give a plausible explanation for the behavior of high frequency AT-cut quartz resonators and dot-resonators on flat wafers. Experimental measurements of inter-resonator coupling and interaction between resonator and wafer edge appear to be in agreement with theory.

Parallel combinations of quartz and ceramic resonators yield a strong zero and pole of impedance corresponding to resonance and antiresonance of the ceramic, a strong zero of impedance corresponding to resonance of the quartz, and a very weak pole contributed by the antiresonance of the quartz. The addition of parallel quartz resonators with appropriately located frequencies to a ceramic ladder filter should yield stable poles of attenuation defining the edge of the pass band without otherwise affecting the pass band behavior. Thickness expander resonators made of hot-pressed ceramic have substantially improved resonant response characteristics at 12 Mc over those using conventionally fabricated ceramic.

CONFERENCES

Date:	18 January 1963	
Place:	Fort Monmouth, New Jersey	
In Attendance:	Dr. R. Bechmann	USAELRDL
	Messrs. E. Gikow	USAELRDL
	A. Rand	USAELRDL
	R. Sproat	USAELRDL
	J. Giannotto	USAELRDL
	D. Koneval	ERD
	P. DiRenzo	ERD
	D. Curran	ERD
Subject:	Progress to date on ceramic and quartz Uni-Wafer filters, design limitations caused by small flaws in ceramic, combinations of quartz and ceramic resonators.	

REPORTS

Thirteenth Monthly Performance Summary
1 December 1962 through 31 December 1962

Fourteenth Monthly Performance Summary
1 January 1963 through 31 January 1963

Fifteenth Monthly Performance Summary
1 February 1963 through 28 February 1963

LIST OF ILLUSTRATIONS

Figure No.

1. Propagation Constants for 10 Possible Modes in AT-Cut Quartz Plate
2. Predominant Particle Displacements for Possible Modes in AT-Cut Quartz Plate
3. Cross-Section AT-Cut Quartz Wafer with Limited Electrode Area
4. Mechanical Coupling Between Closely Spaced Dot-Resonators (3.1b Separation)
5. Mechanical Coupling Between Closely Spaced Dot-Resonators (9.2b Separation)
6. Mechanical Coupling Between Closely Spaced Dot-Resonators (18.5b Separation)
7. Quartz Lattice Filter UWQ-112L (18t Separation-z' Direction)
8. Dot-Resonator Q_m as Function of Distance to Wafer Edge (X-Direction, 1st Run)
9. Dot-Resonator Q_m as Function of Distance to Wafer Edge (X-Direction, 2nd Run)
10. Dot-Resonator Q_m as Function of Distance to Wafer Edge (Z'-Direction, 1st Run)
11. Responses of UWQ-202 Uni-Wafer Ladder Filter and Constituent Dot-Resonators
12. Parallel Combination Quartz and Ceramic Resonators (f_{rq} Less Than f_{rc})
13. Parallel Combination Quartz and Ceramic Resonators (f_{rq} Greater Than f_{rc})
14. Parallel Combination Quartz and Ceramic Resonators (f_{rq} Less Than f_{ac})
15. Parallel Combination Quartz and Ceramic Resonators (f_{rq} Greater Than f_{ac})
16. Seven Dot-Resonator Ceramic Ladder Filter with Single Parallel Quartz Resonator

FERROELECTRIC CERAMIC FILTERS,
IF TRANSFORMERS, AND NETWORKS

Fifth Quarterly Report
1 December 1962 through 28 February 1963

Contract No. DA 36-039 SC-87275

1. FACTUAL DATA

1.1 AT-Cut Quartz Resonators

An explanation is proposed for the behavior of high frequency AT-cut quartz resonators on flat wafers (including range of action) in terms of existing elastic wave theory and the mass loading of electrodes. At 10 Mc and above, AT-cut quartz resonators normally are made using electrodes of limited area and finite thickness on plane wafers. Electrode thicknesses are estimated to be sufficient to lower resonant frequency from 0.1 to 1% below that which would be observed for the unelectroded wafer. Dr. William Shockley, Clevite Palo Alto, predicted that the fundamental thickness shear resonance ω_s for the unelectroded wafer should serve as a cut-off frequency for propagation in the wafer. Existing theory confirmed the existence of this cut-off frequency ω_s for the two of the three principal modes which are excited in AT-cut quartz wafers. Hence, resonance (ω_e) for the electroded portion of the wafer occurs below the cut-off frequency for the plate as a whole ω_s . Therefore at resonance, vibratory energy, which cannot propagate in the unelectroded portions of the wafer, is stored in the electroded portions with energy density decreasing exponentially with distance away from the electrodes. For this reason high Q_m (mechanical) can be achieved with quartz wafers mounted on relatively lossy supports.

Elastic wave theory in AT-cut quartz wafers (monoclinic symmetry) is formidable because of the degree of anisotropy and the resulting interaction between possible modes of vibration. This theory has been the subject of intensive investigation over a period of many years. A notable portion of this work has been performed by R. D. Mindlin and co-workers during the past 12 years. In all of this work interest centered on wave propagation and characteristics of the resulting allowable modes of vibration, with little or no attention paid to cut-off

frequency regions and forbidden modes. It is suggested that precisely opposite emphasis is required for design or understanding of high frequency AT-cut quartz resonators and Uni-Wafer resonator networks.

Solutions to the wave equation, which are appropriate to AT-cut wafers with traction free major surfaces, are of the form

$$u_1 = B_1 e^{-j(\omega t - \xi x_1 - \eta x_3)}, \quad (1)$$

where the indices 1, 2, 3 refer to the rotated crystallographic axes X, Y' (thickness direction), and Z' respectively and u_1 is a displacement in the X direction. The parameters ξ and η are propagation vectors for the X and Z' direction and are given by ω/v . Here v is the appropriate phase velocity which is usually a parameter rather than a constant. When the values of ξ and η are real numbers Eq. (1) describes lossless wave propagation in the x_1 and x_3 directions; when ξ or η is zero it describes an oscillatory vibration which is independent in both amplitude and phase of x_1 or x_3 respectively; and when ξ or η is imaginary it describes an oscillatory vibration which in phase is independent of x_1 or x_3 but in amplitude is an exponentially decreasing function of x_1 or x_3 . Equations for the dependence of the various propagation vectors ξ_i , η_j on frequency and on the physical and dimensional constants of the wafer can be obtained by substituting the 5 component displacement equations (3 linear, 2 rotational) of the form of Eq. (1) in the appropriate wave equations. Consistency requires that the determinants of the coefficients vanish. The roots of the resulting equations, giving propagation vectors as functions of normalized frequency $\Omega = \omega/\omega_s$ for the 10 possible modes of vibration in an AT-cut quartz wafer, were plotted by Mindlin and Gazis,⁽¹⁾ and are reproduced for convenience in Fig. 1. Here the dimensionless wave number is given by $\varphi = \xi b/\pi$ or $\varphi = \eta b/\pi$, where b is wafer thickness. It should be noted that there is a typographical error in Mindlin's Eq. (12), which should read:

(1) R. D. Mindlin and D. C. Gazis, "Strong Resonances of Rectangular AT-Cut Quartz Plates," Final Report June 30, 1961, Contract DA 36-039 SC-87414.

$$(\hat{Y}_{55} \bar{\gamma}^2 - \Omega^2)(\hat{C}_{55} \bar{\gamma}^2 - 3\Omega^2 + 3) = 0 \quad (2)$$

Excellent graphic descriptions of the 10 modes of vibration are also given by Mindlin and Gazis. These are reproduced for convenience in Fig. 2.

While there are 10 possible modes, only three principal modes are strongly excited in AT-cut quartz wafers with limited electrode areas. These are TS_1 (thickness shear mode) and F_1 (flexural mode) which propagate in the X direction, and TT_3 (thickness twist mode) which propagates in the Z' direction. Of these, both TS_1 and TT_3 have cut-off frequencies at $\omega = \omega_s$, which means that these modes will not propagate in the unelectroded plate for $\omega < \omega_s$, but rather will have amplitudes which decrease exponentially in the X and Z' directions respectively. On the other hand F_1 has no cut-off frequency and will propagate in the X direction. However, it should be closely coupled to the TS_1 mode and therefore should in effect have a complex propagation constant, i. e., with an amplitude decreasing exponentially with distance in the X direction. It is assumed that wave propagation in any arbitrary direction in the XZ' plane could be resolved into X and Z' components and therefore would be similarly attenuated for $\omega < \omega_s$. Therefore in an ideal lossless wafer, if one portion is driven in the thickness shear mode at frequencies less than ω_s , the resulting vibratory energy will not propagate away from the driven portion to any appreciable extent, but rather will be stored in and around the driven portion of the wafer.

The cross-section of a dot-resonator on a large wafer, or, for that matter, any high frequency AT-cut quartz resonator, is similar to that sketched in Fig. 3. Typically it would consist of a pair of small circular electrodes of diameter d_e and thickness τ_e , which is exaggerated for clarity. Additional deposited conducting strips (not shown) are used for making electrical contact with the resonator electrodes. Quartz crystal resonators are normally made somewhat thinner, i. e., higher in frequency, than is desired and then back plated (reduced in resonant frequency) by increasing the thickness of the electrodes τ_e . This is done not only for convenience in fabrication but also to reduce resonant resistance and to improve the overall resonator response. The proposed

mathematical model offers a qualitative explanation for this behavior and for some specific situations a quantitative one.

This model is based on one important assumption: that elastic wave theory for flat plates of uniform cross-section applies to good approximation to quartz wafers only partially covered with thin electrodes. In effect, this assumes that the discontinuity at the edge of the electrode is so slight that the resulting perturbation to elastic wave propagation is negligible. The AT-cut quartz resonators just described usually have very thin electrodes as is evidenced by resonant frequencies ω_e from 0.1 to 1% below that of the unelectroded wafer, i. e., $\Omega_o = \omega_e / \omega_s = 0.99$ to 0.999.

For the TT_3 mode in the Z' direction, the propagation vector is obtained from Eq. (2) in terms of wafer thicknesses b :

$$b\beta = j\pi [(1 - \Omega^2) c_{66} / c_{55}]^{1/2}, \quad (3)$$

where the ratio of elastic modulii $c_{55} / c_{66} = 2.37$ for quartz. From this and Eq. (1), the spatial distribution of vibratory energy (TT_3) in the unelectroded portion of the wafer, observed in the Z' direction with the edge of the electrode chosen as the origin, is of the form

$$E_{TT3} = E_o e^{j2\beta x_3} = E_o e^{-2\pi [(1 - \Omega^2)/2.37]^{1/2} (x_3/b)}. \quad (4)$$

As an example, for $\Omega_o = 0.99$ this would give at resonance an attenuation coefficient for energy density of 2.5 db/wafer thickness and for $\Omega_o = 0.999$, of 0.79 db/wafer thickness. It should be noted that attenuation, as described here, does not denote energy dissipation but merely the spatial distribution of stored energy.

Smaller values of Ω_o will therefore result in a concentration of a larger fraction of the total vibratory energy in and around the electroded area of the wafer, i. e., less fringing energy available for other portions of the wafer. With all other factors being equal, the resonator with the lower value of Ω_o should have the higher value of mechanical Q. Similarly, the interference between one electroded area (dot-resonator) and another, or an edge of the wafer is a function

not only of distance separating them but also of Ω_0 , where the resonator with the lower value of Ω_0 will have the shorter range of influence. In this case, specific attenuation levels can be obtained for given values of Ω and distance.

1.2 Experimental Evaluation of Range of Action for Quartz Dot-Resonators

Progress was made toward an experimental evaluation of "range of action" for dot-resonators in Uni-Wafer filters before and during the analysis described in Section 1.1. Range of action has been loosely defined as the distance within which a physical disturbance or discontinuity, e. g., edge of the wafer, would noticeably affect the response of a dot-resonator. This was previously investigated (Fourth Quarterly Report) in terms of the interaction between pairs of resonators which formed the two arms of a half lattice filter. These measurements gave only qualitative data.

These same filter wafers, each of which consists of a pair of resonators with the resonant frequency of the one tuned to the antiresonant frequency of the other, have now been examined as electromechanical filters. These filter wafers, designated UWQ-115L, 114L, and 112L, have resonators separated in the Z' direction by 3.1b, 9.2b, and 18.5b respectively. (The wafer thickness b equals 6.5 mils for 10 Mc AT-cut quartz wafers.) With resistive matched source and load, one of the resonators was electrically driven, while the response was observed across the second. For separations of 3b and 9b, the resonant frequency of the first or driven resonator coincided with the antiresonant frequency of the second. However, the third filter (18b) was inadvertently measured in the reverse direction. In all cases a recognizable pass band was observed in which the center frequency coincided with that previously obtained for these units operated as half lattice filters. Figures 4, 5, and 6, give the response curves of these units both with and without electrical shielding. In the former case, minimum insertion losses of 6 db, 21 db and 40 db were observed for the principal passbands with respective resonator separations of 3b, 9b, and 18b, whereas these same units had less than 1 db insertion loss as lattice filters.*

* Figure 7 is included from the Fourth Quarterly Report as a comparison of the lattice filter response of UWQ-112L, i. e. resonators separated by 18b.

The minimum insertion loss in the principal pass band in Figs. 4, 5, and 6, i. e., increasing loss with increasing separation, was anticipated from previous observations with quartz and ceramic resonators; however, the strong spurious responses above the principal pass band were not. Their existence is plausible in view of the fact that they occur above the cut-off frequency ω_s for the wafer, i. e., in the frequency range where attenuation free propagation occurs. They are probably the result of lateral standing wave patterns involving the two dot-resonators and at least a portion of the disk as a whole.

The minimum insertion losses for the principal pass bands of the three filters were used to calculate attenuation constants with the assumption that all of the observed loss could be attributed to cut-off region attenuation as predicted from Eq. (4).

$$\alpha = 10 \log_{10} e^{-2Yx}, \quad (5)$$

where α = attenuation in db,

$Y = -j\beta$ = attenuation constant

x = separation between dot-resonators (between edges of electrodes).

The resulting values are listed in Table I along with the corresponding theoretical values of ω_e/ω_s obtained from Eq. (3).

Table I. Attenuation Constants from UWQ-115L, 114L, and 112L.

Filter Number	Dot-Resonator Separation	Minimum Insertion Loss	Y_b	ω_e/ω_s (theoretical est.)
UWQ				
115L	3.1b	6 db	0.22	0.9936
114L	9.2b	21	0.26	0.9912
112L	18.5b	40	0.25	0.9919

At present, instrumentation is not available to measure electrode thickness and/or w_e/w_s . However, the values of w_e/w_s correspond roughly in magnitude to those which would be obtained from previous estimates of electrode thickness, e.g., of the order of 10 microinches for electroless silver deposits.

A second set of experiments were initiated to investigate "range of action" in terms of the more limited definition as that distance within which a physical discontinuity will measurably affect the response of a dot-resonator. Initially, it was planned to observe both the number and magnitude of spurious responses as well as the resonator mechanical Q , as a function of the distance from the electrode to the nearest edge of the wafer in both the X and Z' directions. Preliminary measurements taken in the X direction indicated that Q_m is by far the more sensitive indicator and, hence, suggested the feasibility of a quantitative definition of the range of action in terms of Q_m and the electrode to wafer edge separation.

In all, four quartz resonators were prepared in which the initial separation between the dot-electrode and the nearest wafer edge was greater than the minimum derived from the criteria of Bechmann⁽²⁾ for clean responses in high frequency AT-cut quartz disk shaped resonators. The wafers were not necessarily regular in shape, nor were the electrodes symmetrically positioned with respect to the wafer boundaries. For each of these units, the electrode to edge separation was reduced step wise by removing portions of a wafer edge using a small (0.125") coated mandrel type diamond drill. The characteristic frequencies and impedances were measured and mechanical Q_m calculated after each incremental change. The results for the first unit were inconclusive due to a non-continuous electrode lead. The air dry silver connection used to repair the broken lead somewhat damped the crystal response and resulted in a low initial Q_m value. In the process of making the measurements some of the air dry silver flaked off, decreasing the damping and causing a corresponding increase in Q_m which masked any change due to varying the electrode to edge separation. The first spurious response (~ 0.2 db) was observed for a separation of approximately

⁽²⁾ R. Bechmann, "Quartz AT-Type Filter Crystals for the Frequency Range 0.7 to 60 Mc," Proceedings of the IRE, Vol. 49, No. 2, pp. 523-524 (1961).

5b. At this point the crystal was broken in attempting to continue the measurements.

The remaining three units had essentially constant Q_m values in excess of 100,000 for large electrode to edge separations. As separation was decreased, Q_m decreased slowly to a turning point or knee in the curve, below which Q_m decreased more rapidly with decreasing distance. The knee in the curves for the two sets of data in the X direction, Figs. 8 and 9, appear to fall between 8b and 14b (wafer thickness b); in the Z' direction, Fig. 10, the knee occurs between 4b and 7b. Dr. Shockley suggested that a functional dependence could be more readily obtained if the numerical data were first plotted as $1/Q_m$. Functional dependence of the form

$$\frac{1}{Q_m} = \delta_1 e^{-2Yd} + \delta_2 \quad (6)$$

was found to fit the three sets of data closely as can be seen in Figs. 8 to 10, where the solid curves were plotted using the parameters listed in Table II.

Table II. Experimental Parameter Evaluation for Eq. (6).

Direction	Yb	δ_1	δ_2
X	0.23	1.6×10^{-4}	8.9×10^{-6}
X	0.18	2.0×10^{-4}	9.6×10^{-6}
Z'	0.29	1.8×10^{-4}	9.0×10^{-6}

The functional dependence of Eq. (6) is in agreement with the theoretical outline of Section 1.1 if the loss factor δ_1 , considered to be the overall loss factor associated with the diamond ground edge, can be lumped in one constant and if the factor δ_2 is assumed to be the value, $1/Q_m$, which would be observed for the same dot-resonator on an infinite wafer. It is gratifying to note that the values of propagation constant listed in Table II are also comparable in magnitude to those which would be calculated from the estimated thicknesses of electroless silver electrodes.

1.3 Higher Frequency Quartz Resonators and Filters

A 20-Mc resonator was fabricated which had a resonant resistance of 40 ohms, a $\Delta f = 29$ kc and correspondingly a $Q \sim 80,000$. This unit differed from that of previous resonators in that the electrode configuration consisted of two strip electrodes, one on the top surface of the wafer, the other oriented at right angles to the first, on the bottom surface of the wafer, i.e., a cross. The strip electrodes were approximately $0.050'' \times .5''$, hence, at the point of coincidence, a square electrode measuring $\sim 0.050''$ on a side was obtained. Such an electrode configuration may be of value at higher frequencies where increasingly smaller electrode areas are required to maintain spurious free resonator responses. At these frequencies, a multi-resonator Uni-Wafer filter could conceivably consist of a series of line electrodes properly orientated on the top and bottom surfaces of the crystal.

A 20 Mc AT-cut Uni-Wafer ladder filter consisting of 5 dot-resonators was also fabricated. The resonators had electroless silver electrodes of the conventional type, i.e., $0.050''$ diameter electrodes with appropriate electrode leads. The responses of the individual tuned resonators are shown in Fig. 11. The response of the resultant filter is also shown in Fig. 11. This unit had 3, 6, 10 and 20 db bandwidths of 65, 77, 80 and 85 kc respectively and an overall stopband rejection of about 14 db.

1.4 Combinations of Quartz and Ceramic Resonators

Ceramic and quartz resonator filters have, by nature, distinctly different characteristics. For the most part quartz filters are extremely stable narrow bandwidth devices and are relatively expensive. On the other hand, ceramic filters are wide bandwidth devices with moderate stability and low to moderate cost. It was proposed to investigate the feasibility of filters using both quartz and ceramic resonators and hopefully combining the better features of each.

Compared with quartz, ceramic resonators have considerably larger coupling coefficients .4 vs .1, dielectric constants 1000 and 450 vs 4, and mechanical and electrical loss factors of the order of 10^{-3} vs 10^{-6} . Because of these large differences, combinations of quartz and ceramic resonators should be possible which selectively emphasize specific characteristics. The simplest of these is the parallel combination of single ceramic and quartz resonators. In

this case a strong zero and pole of impedance corresponding to f_{rc} and f_{ac} for the ceramic resonator should be obtained along with a strong zero at f_{rq} for the quartz. The pole of impedance corresponding to f_{aq} should be very weak because of the parallel combination of a relatively large lossy capacitor (C_{oc} of the ceramic resonator).

Parallel combination of single quartz and ceramic resonators confirmed these predictions for quartz resonators with f_{rq} located 30 kc below f_{rc} (Fig. 12), 30 kc above f_{rc} (Fig. 13), 50 kc below f_{ac} (Fig. 14), and 50 kc above f_{ac} (Fig. 15). In each of these cases, f_{rc} and f_{ac} were essentially unchanged by the addition of the quartz resonator, and f_{rq} coincided with that of the quartz resonator alone. It should be noted in Figs. 13 and 14, where f_{rq} falls between f_{rc} and f_{ac} , that the weak antiresonance associated with the quartz resonator occurs below its resonance.

From these data it would appear that several quartz resonators could be used as parallel elements to "stake down" the edges of the pass band in a ceramic ladder filter by providing invariant poles of attenuation with the inherent stability of quartz resonators without otherwise affecting the ceramic pass band. A 7 dot-resonator ceramic ladder filter with a single quartz resonator connected in parallel resulted in a single "pole" of attenuation at f_{rq} as shown in Fig. 16 without appreciably changing the remainder of the pass band. From this it is concluded that the use of several parallel quartz resonators, with f_{rq} values staggered slightly at each edge of the pass band, should define a stable pass band in a ceramic filter and should also provide sharp corners at the cut-off frequencies. Neither of these features can be provided by ceramic resonators alone.

Series combinations of single quartz and ceramic resonators were also investigated. In this case the high impedance level of the quartz resonator totally masked the response of the ceramic resonator so that the resultant was essentially equivalent to the response of a quartz resonator alone.

1.5 Ceramic Resonators

Considerable difficulty has been encountered in attempts to achieve good ceramic thickness resonators in the 10 Mc region. This has been attributed to the existence of many small holes in conventionally prepared PZT* -6 ceramic.

^{*} Reg. U.S. Pat. Off.

In attempts to avoid this, slip-cast and hot-pressed fabrication techniques are being investigated. First fragmentary pieces of hot-pressed PZT-6A ceramic appeared to be free of these holes or flaws. These have been fabricated into 12 Mc dot-resonators with encouraging results. Six irregularly shaped platelets with 1/16" diameter electroless silver electrodes were tested as thickness expander resonators. Since the electrodes were apparently not an optimum size, all resonators had spurious responses. However, four of them had sufficiently well defined responses to obtain the Q_m values listed in Table III.

Table III. Q_m Measurements for Thickness Expander Resonators Made of Hot-Pressed PZT-6A Ceramic

Number	f_r	Δf	C_e	Q_m
2	11.935 Mc	230 kc	90 pf	395
3	11.988	240	74	475
5	12.213	317	90	300
6	11.799	135	90	440

These values of Q_m , which because of spurious responses should be considered only as lower bounds, are higher by more than a factor of 2 over those usually achieved with commercially available PZT-6A ceramic sheet stock ($Q_m \approx 150$, $\Delta f \approx 300-500$ kc at 11 Mc) in the thickness expander mode. Additional pieces of hot-pressed PZT-6A and 6B ceramic are now in process.

2. CONCLUSIONS

A theoretical explanation has been outlined for the behavior of high frequency AT-cut quartz resonators on flat wafers in terms of existing elastic wave theory and the mass loading of the electrodes. It is proposed that the mass loading of the electrodes lowers the resonant frequency of the resonator ω_e to slightly below that of the unelectroded wafer ω_s which also serves as a cut-off frequency for propagation of 2 out of 3 principal modes in the plane of the wafer. Therefore, vibratory energy is concentrated in the region in and around the electroded portion.

This gives a plausible explanation for high Q_m observed in flat plate resonators and also provides a theoretical basis for range of action and Uni-Wafer filter design. Experimental data on inter-resonator coupling and the interaction between resonator and wafer edge appear to be in agreement with theory, although direct confirmation has not yet been obtained. It is anticipated that substantial improvements in high frequency quartz resonator design should result from the application of the principles outlined in theory.

Parallel combinations of quartz and ceramic resonators yield a strong zero and pole of impedance corresponding to the resonance and antiresonance of the ceramic, a strong zero corresponding to the resonance of the quartz, and a very weak pole contributed by the antiresonance of the quartz (but considerably altered in frequency). The addition of parallel quartz resonators in ceramic ladder filters can yield stable poles of attenuation defining the edges of the pass band without otherwise affecting the pass band.

3. PLANS FOR NEXT INTERVAL

Experimental confirmation of theoretically predicted behavior will be attempted using dot-resonators with controlled-thickness evaporated silver electrodes. This will include inter-resonator coupling and resonator to wafer edge interaction experiments. A variable air gap measurements jig will be designed and constructed using micrometer heads so that existing electrode thicknesses might be calculated and so that resonator characteristics of unelectroded wafers could also be measured. Evaluation of ceramic resonators fabricated from hot-pressed and slip-cast ceramic will be conducted in an attempt to obtain suitable material for ceramic filter samples.

4. **IDENTIFICATION OF KEY TECHNICAL PERSONNEL**

The time devoted in this project by principal technical personnel and others during the period from 1 December 1962 through 28 February 1963 follows:

<u>Personnel</u>	<u>Man-Hours</u>
A. Berohn	410
D. Curran	202
D. Koneval	428
Others	20
Total	1060

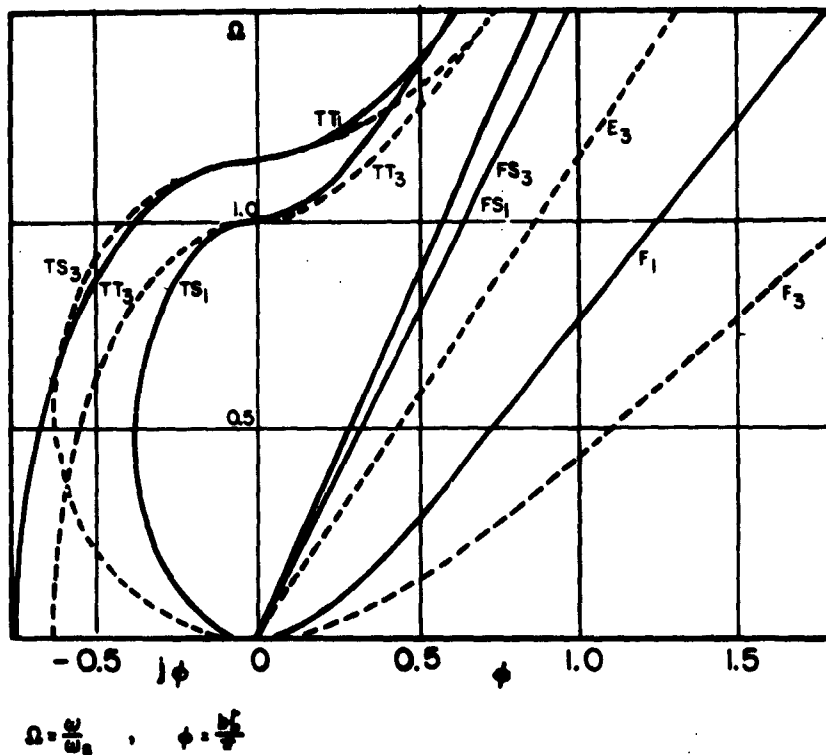
5. INITIAL DISTRIBUTION

Copy No.

1. Electronic Research Division (H. Jaffe)
2. Electronic Research Division (Project Administration)
3. Clevite Patent Department
- 4-6. Clevite Library
7. Electronic Research Division (D. Curran)
8. Electronic Research Division (D. Koneval)
9. Electronic Research Division (W. Gerber)
10. Electronic Research Division (A. Waren)
11. Electronic Research Division (J. Koenig)
- 12-15. Electronic Research Division
16. Clevite Piezoelectric Division (J. Arndt)
17. Clevite Piezoelectric Division (A. Lungo)
18. Clevite Transistor (M. J. Fleming, Jr.)
19. Shockley Transistor (Dr. W. Shockley)
20. Brush Crystal, Ltd.
Hythe-Southampton
England
Attn: Mr. Norman Hunt
- 21-22. Review Copies
Chief, Microwave and Inductive Devices Branch
Electronic Parts and Materials Division
Electronic Components Research Department, USASRDL
- 23-82. USAELRDL Distribution List

FIGURE I. PROPAGATION CONSTANTS FOR TEN POSSIBLE MODES IN AT-CUT QUARTZ PLATE.

(AFTER MINDLIN AND GAZIS, SIGNAL CORPS
CONTRACT DA36-039 SC-87414, JUNE, 1961)



TT = THICKNESS - TWIST
TS = THICKNESS - SHEAR
E = EXTENTION
FS = FACE - SHEAR
F = FLEXURE

FIGURE 2.

PREDOMINANT PARTICLE DISPLACEMENTS FOR POSSIBLE MODES
IN A T-CUT QUARTZ PLATE. (AFTER MINDLIN AND GAZIS,
SIGNAL CORPS CONTRACT DA 36-039 SC-87414, JUNE, 1961)

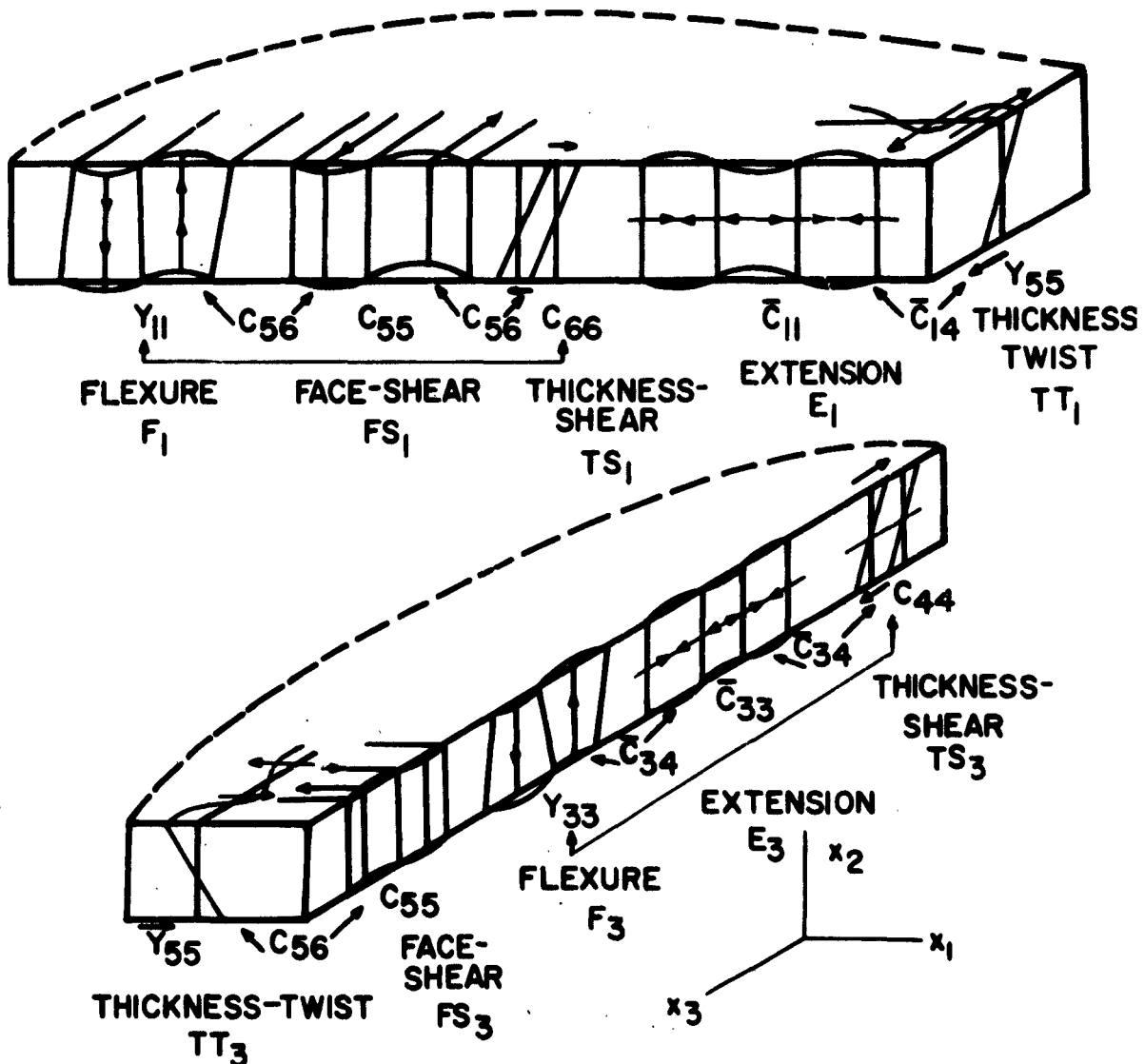


FIGURE 3. CROSS-SECTION AT-CUT QUARTZ WAFER
WITH LIMITED ELECTRODE AREA.

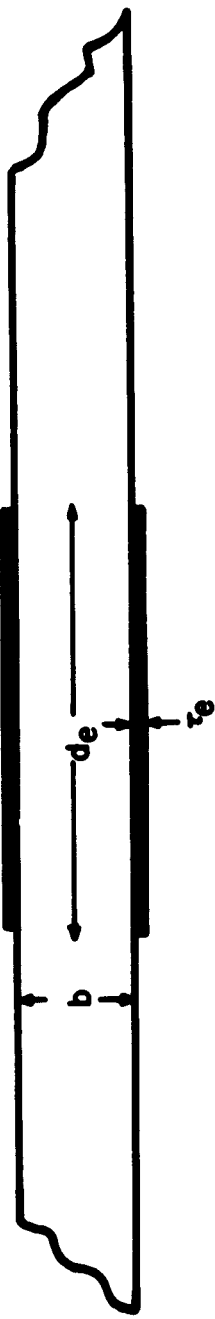
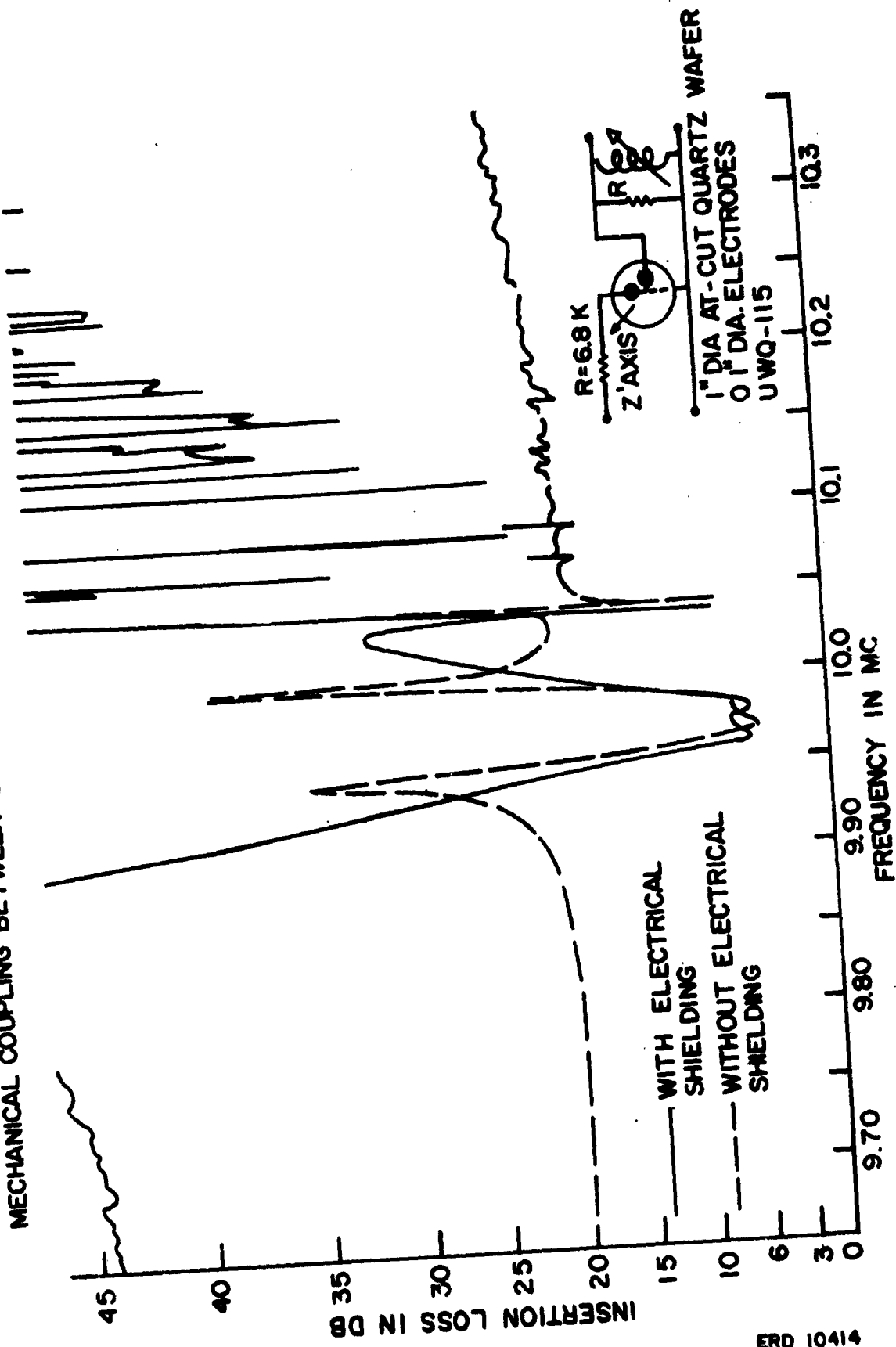
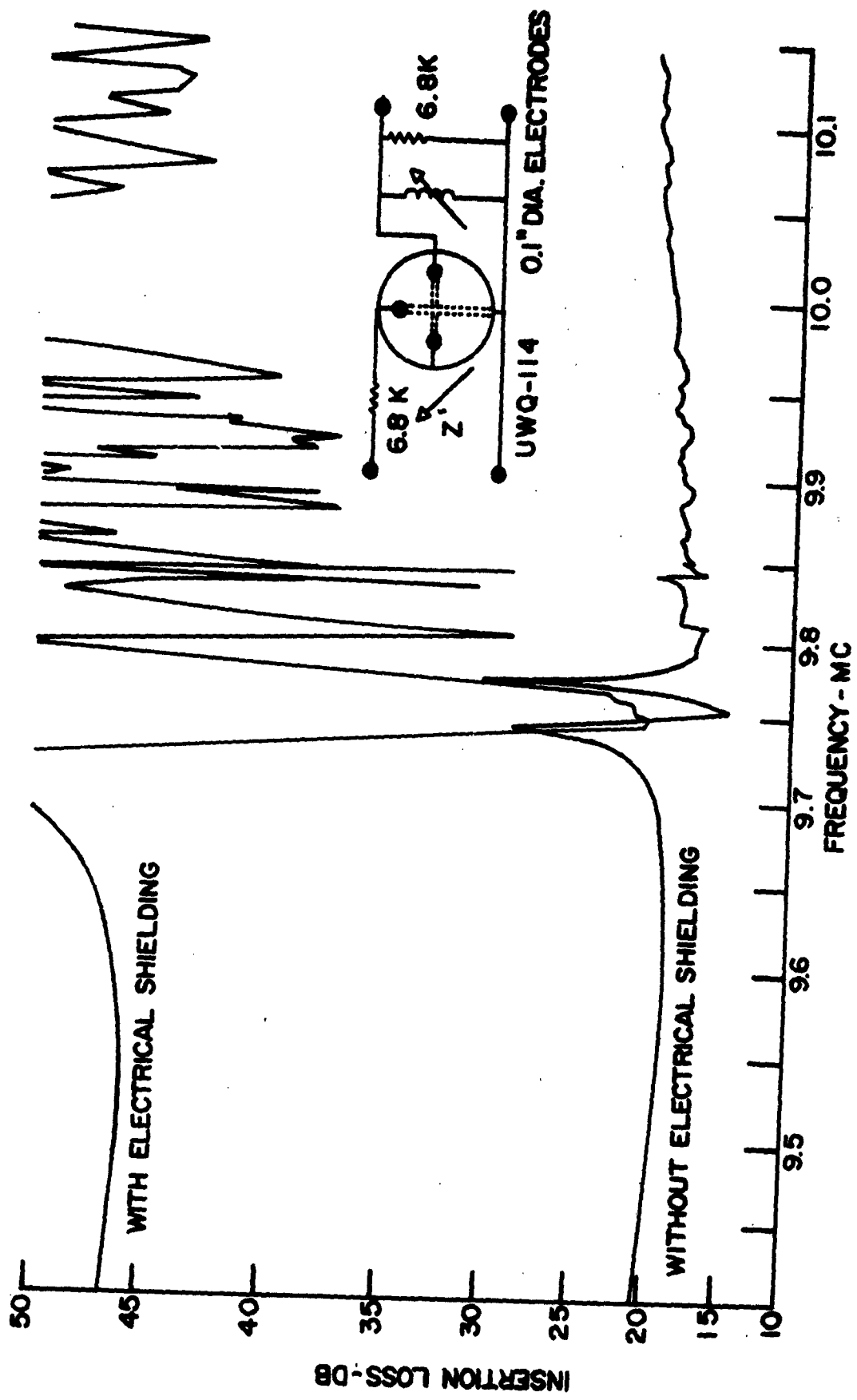


FIGURE 4.
MECHANICAL COUPLING BETWEEN CLOSELY SPACED DOT-RESONATORS (3.1b SEPARATION)



ERD 10414

FIGURE 5.
MECHANICAL COUPLING BETWEEN CLOSELY SPACED DOT-RESONATORS (9.2b SEPARATION)



ERD 10441

FIG. 6. MECHANICAL COUPLING BETWEEN CLOSELY SPACED DOT-RESONATORS (18.5b SEPARATION)

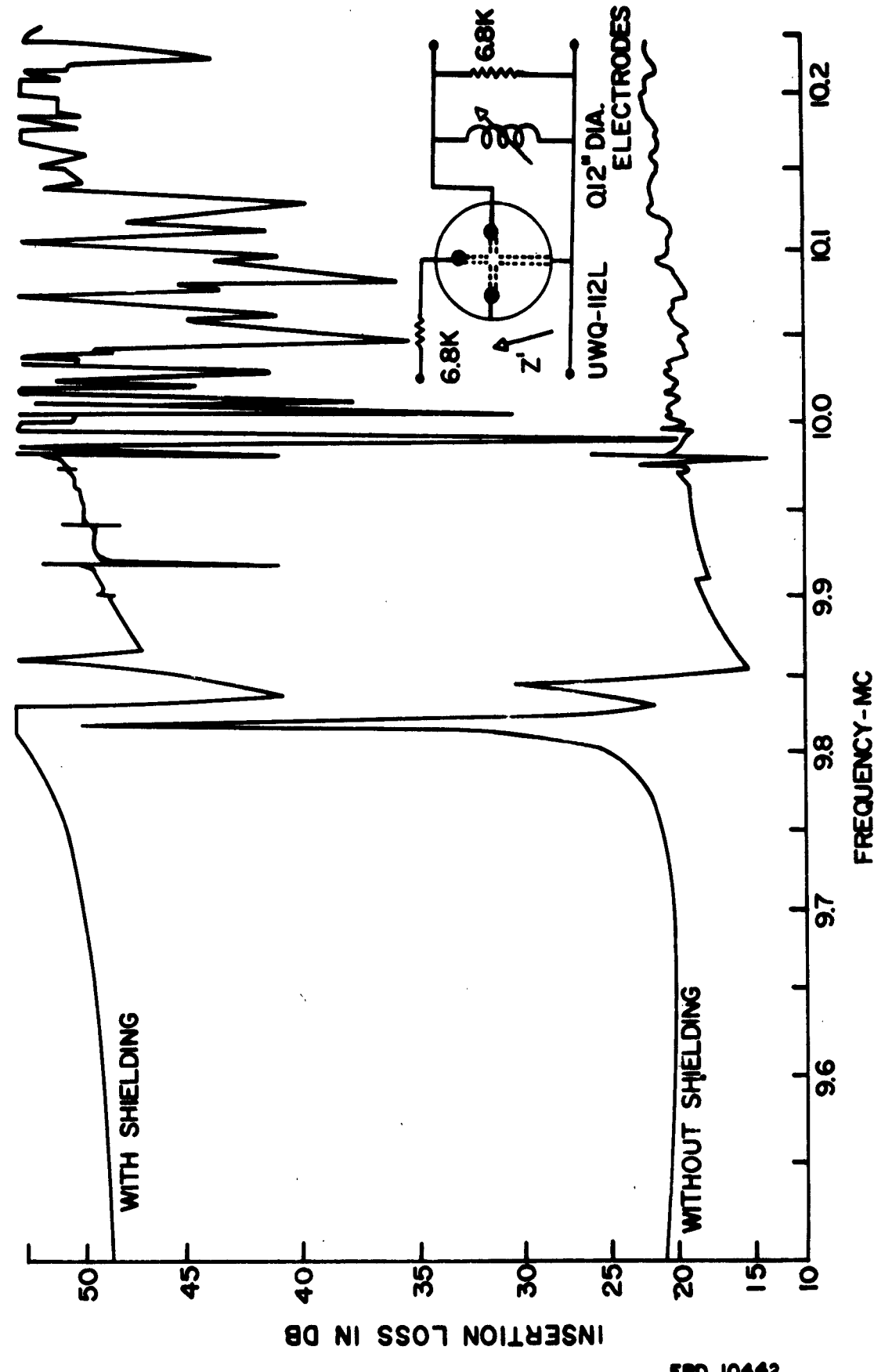
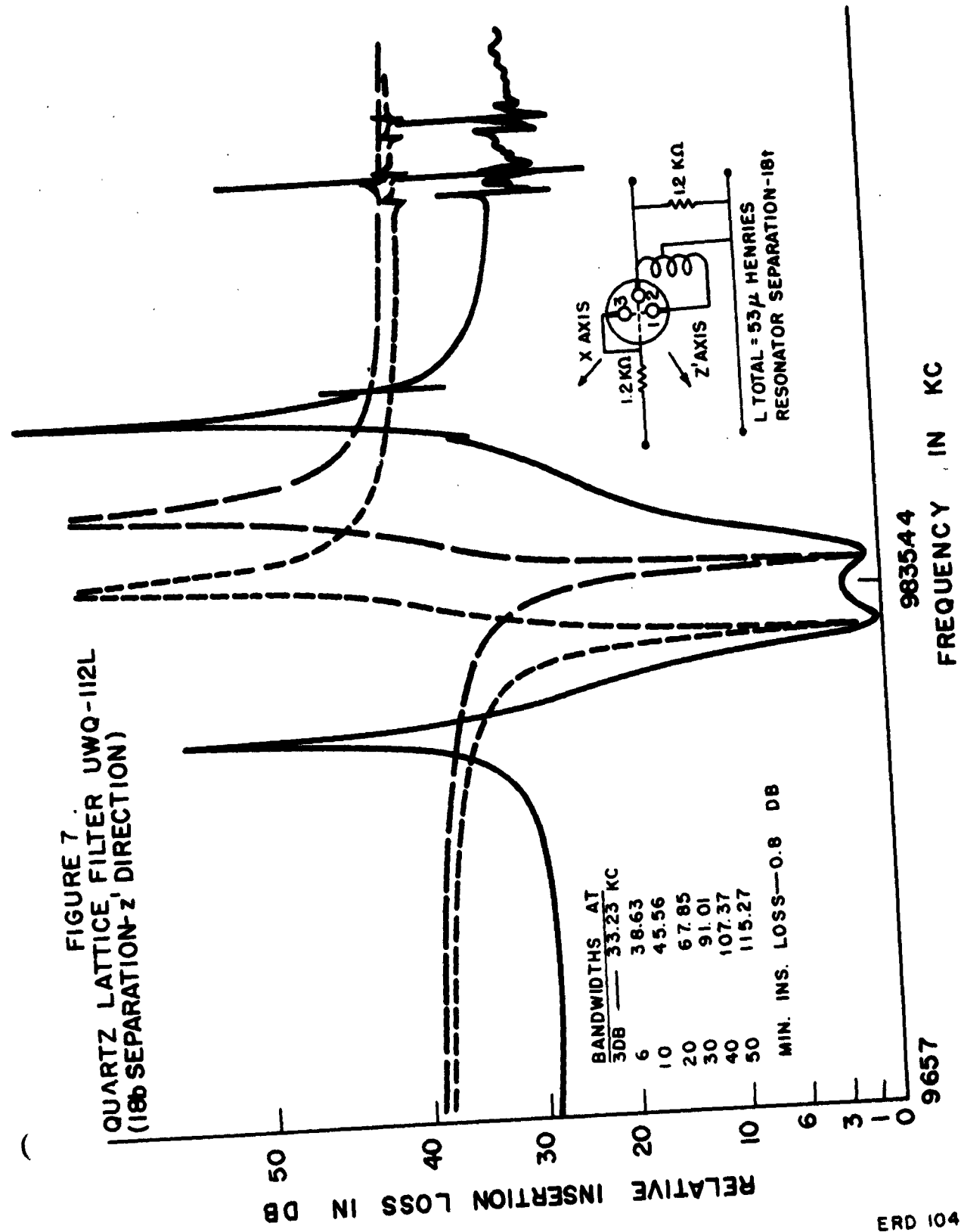
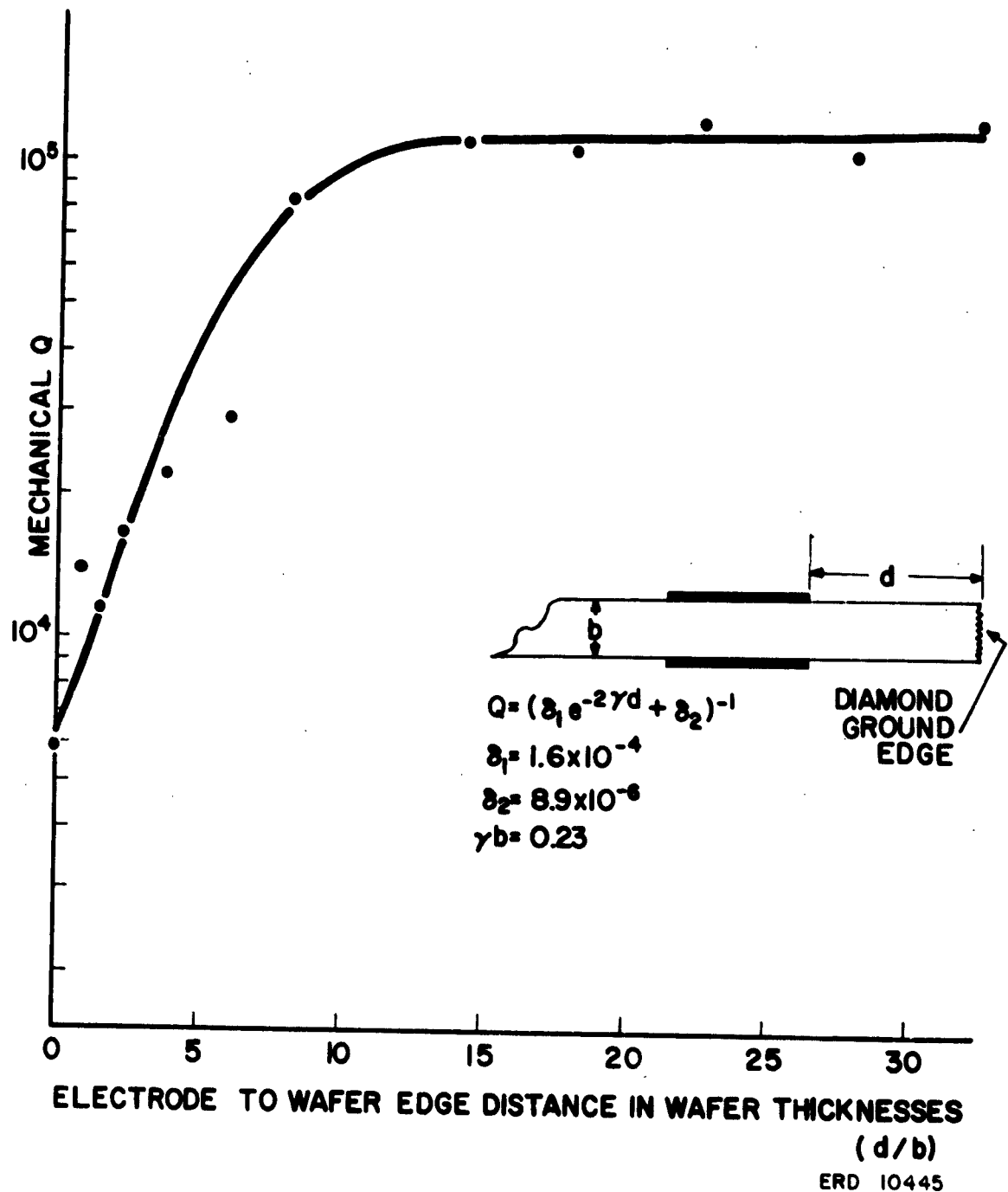


FIGURE 7. LATTICE FILTER UWO-112L
 QUARTZ (180° SEPARATION-z DIRECTION)



ERD 10422

FIGURE 8. DOT-RESONATOR Q_m AS FUNCTION OF DISTANCE
TO WAFER EDGE (X-DIRECTION, 1st RUN).



ERD 10445

FIGURE 9. DOT-RESONATOR Q_m AS FUNCTION OF DISTANCE
TO WAFER EDGE (X-DIRECTION, 2nd RUN).

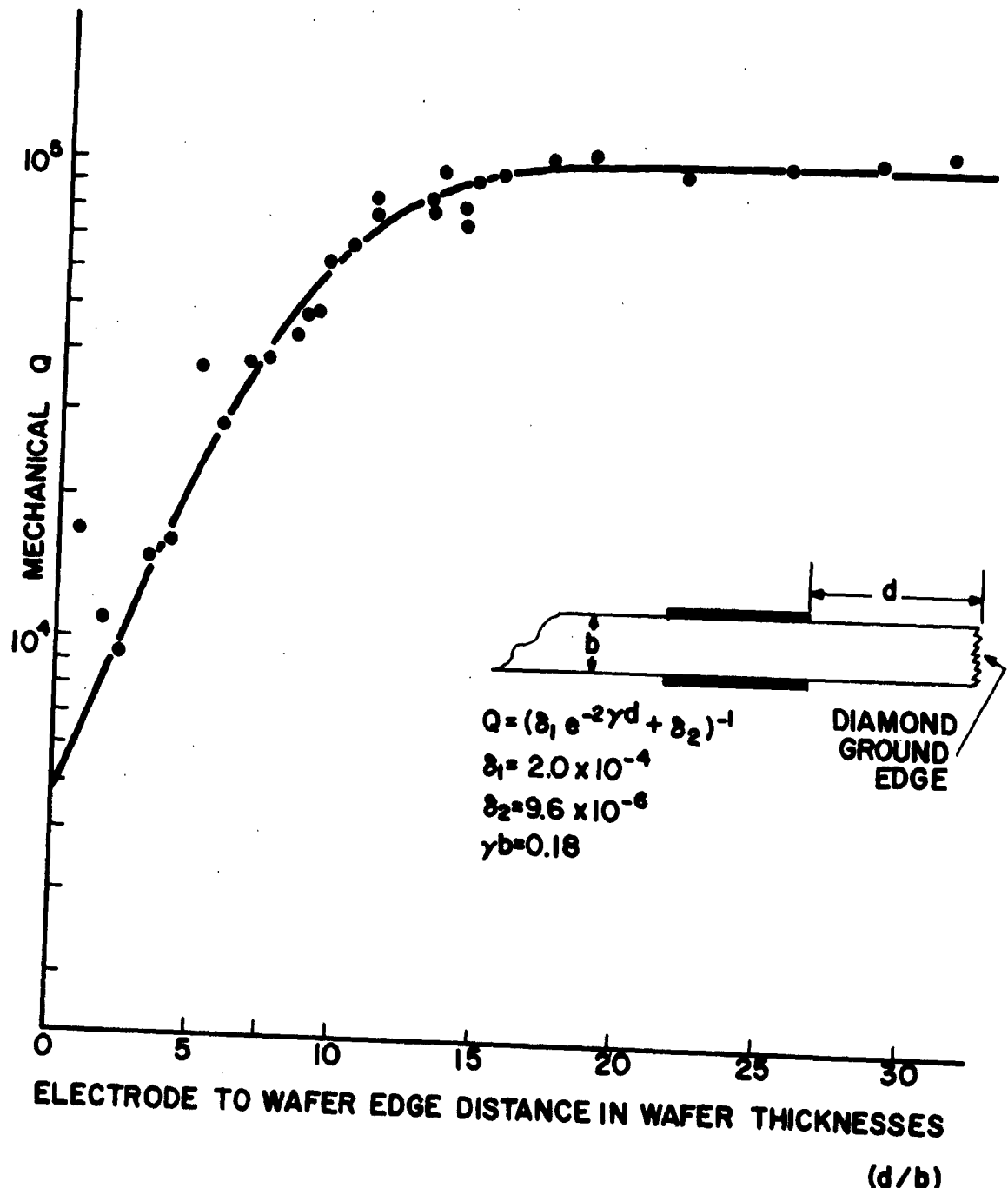


FIGURE 10. DOT-RESONATOR Q_m AS FUNCTION OF DISTANCE
TO WAFER EDGE (Z'-DIRECTION 1st RUN).

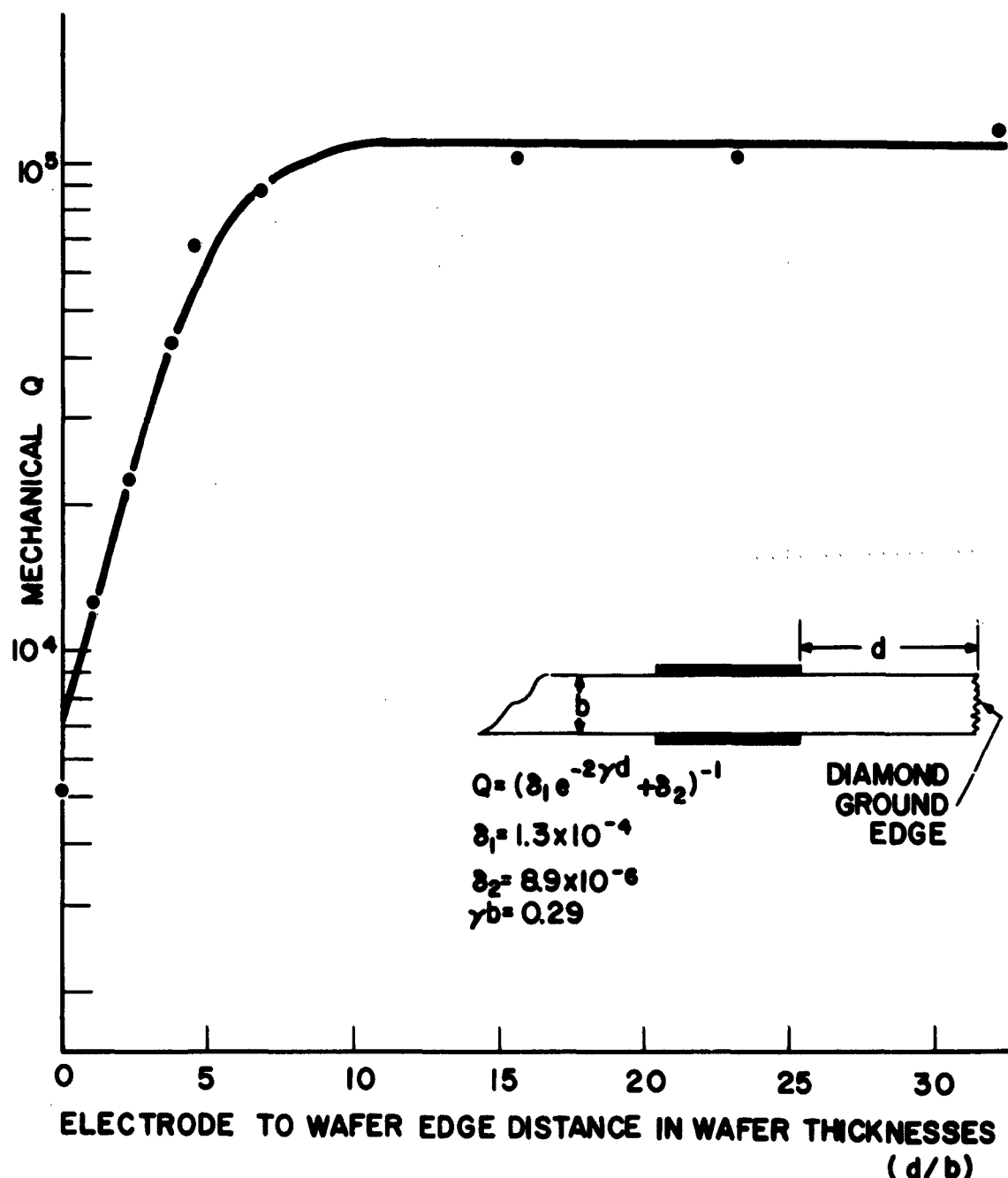


FIGURE II. RESPONSES OF UWO-202 UNI-WAFER LADDER FILTER
AND CONSTITUENT DOT-RESONATORS

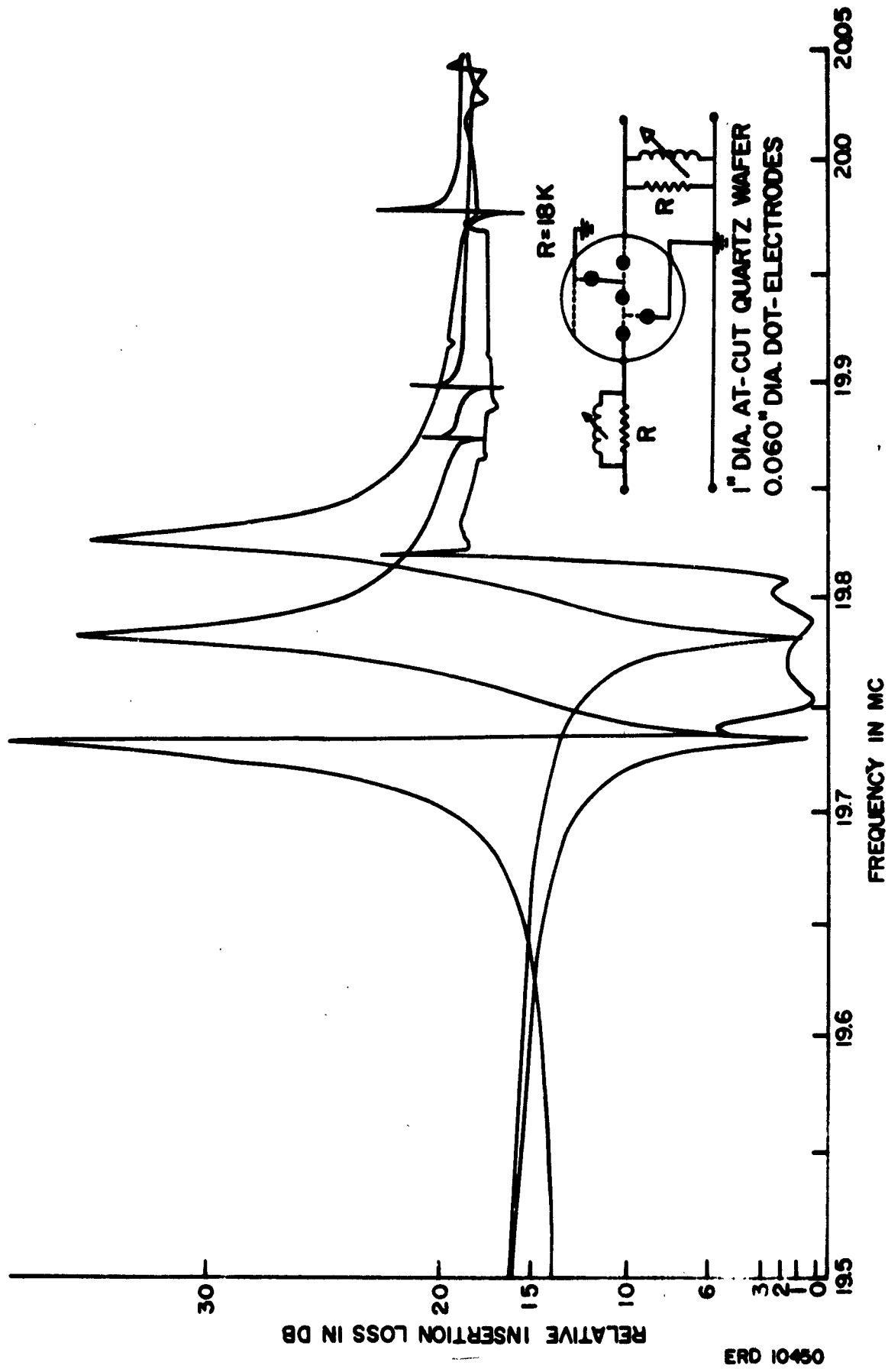
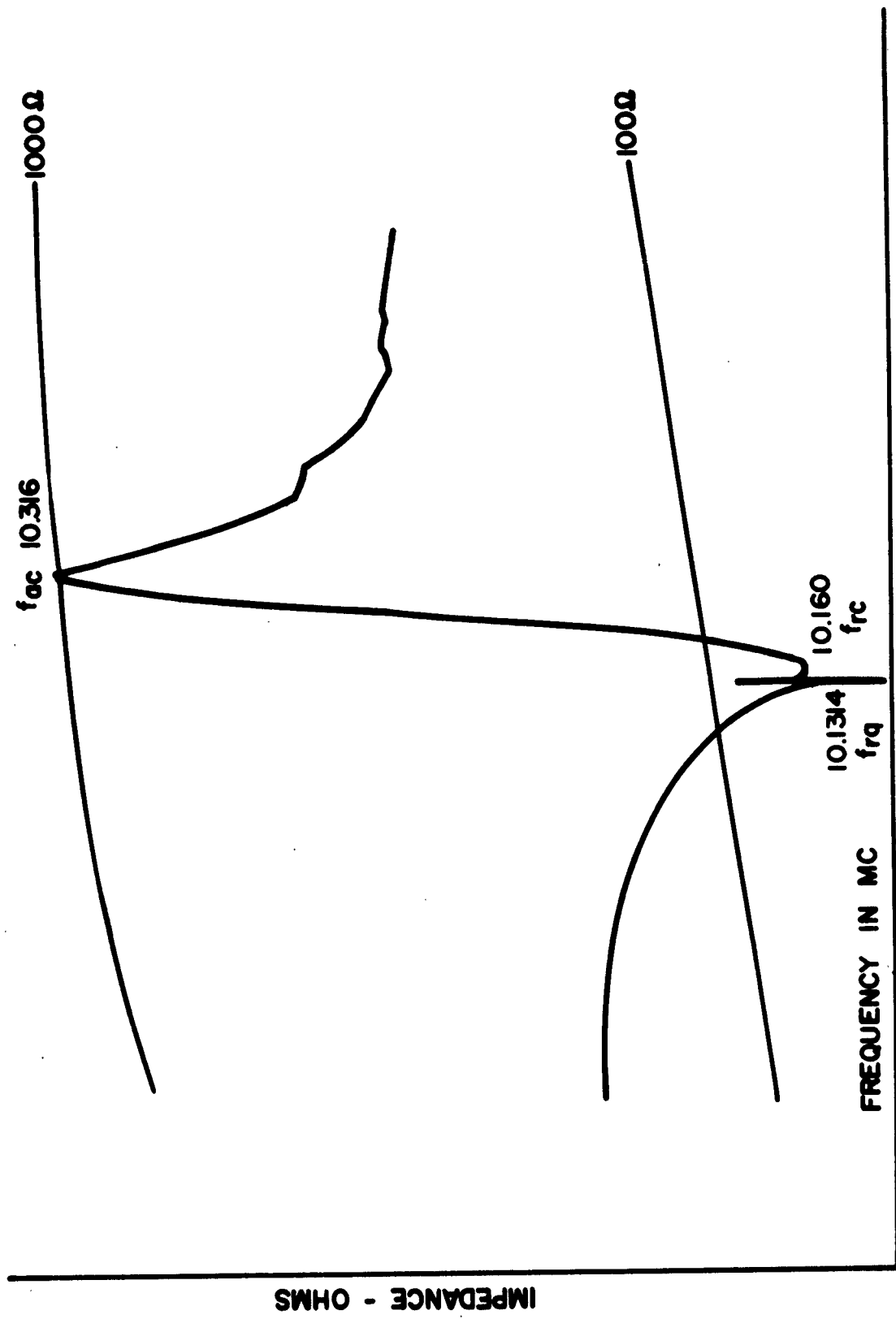
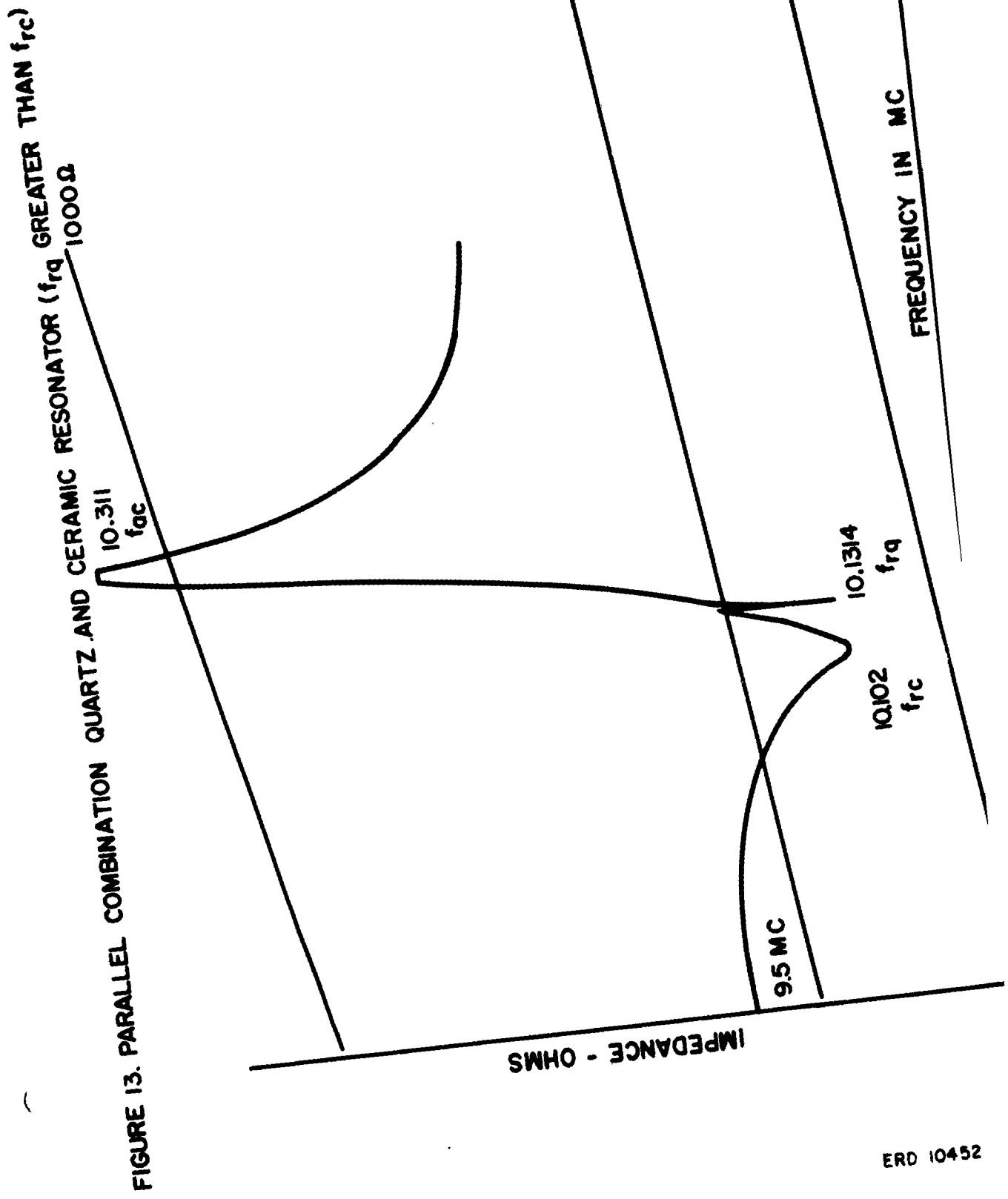


FIGURE 12. PARALLEL COMBINATION QUARTZ AND CERAMIC RESONATORS (f_{rq} LESS THAN f_{rc}).





ERD 10452

FIGURE 14. PARALLEL COMBINATION QUARTZ AND
CERAMIC RESONATORS (f_{rq} LESS THAN f_{qc}).

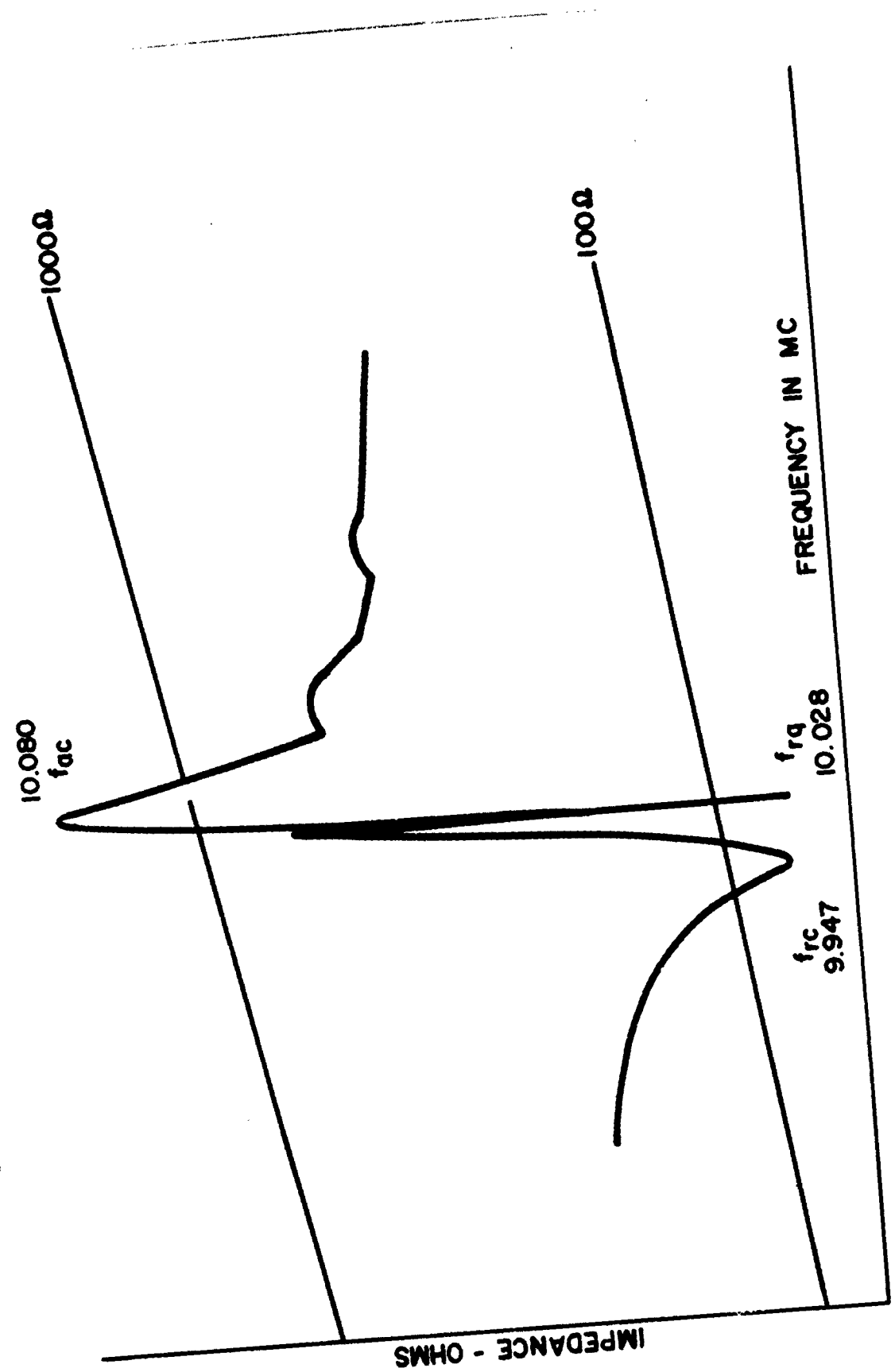
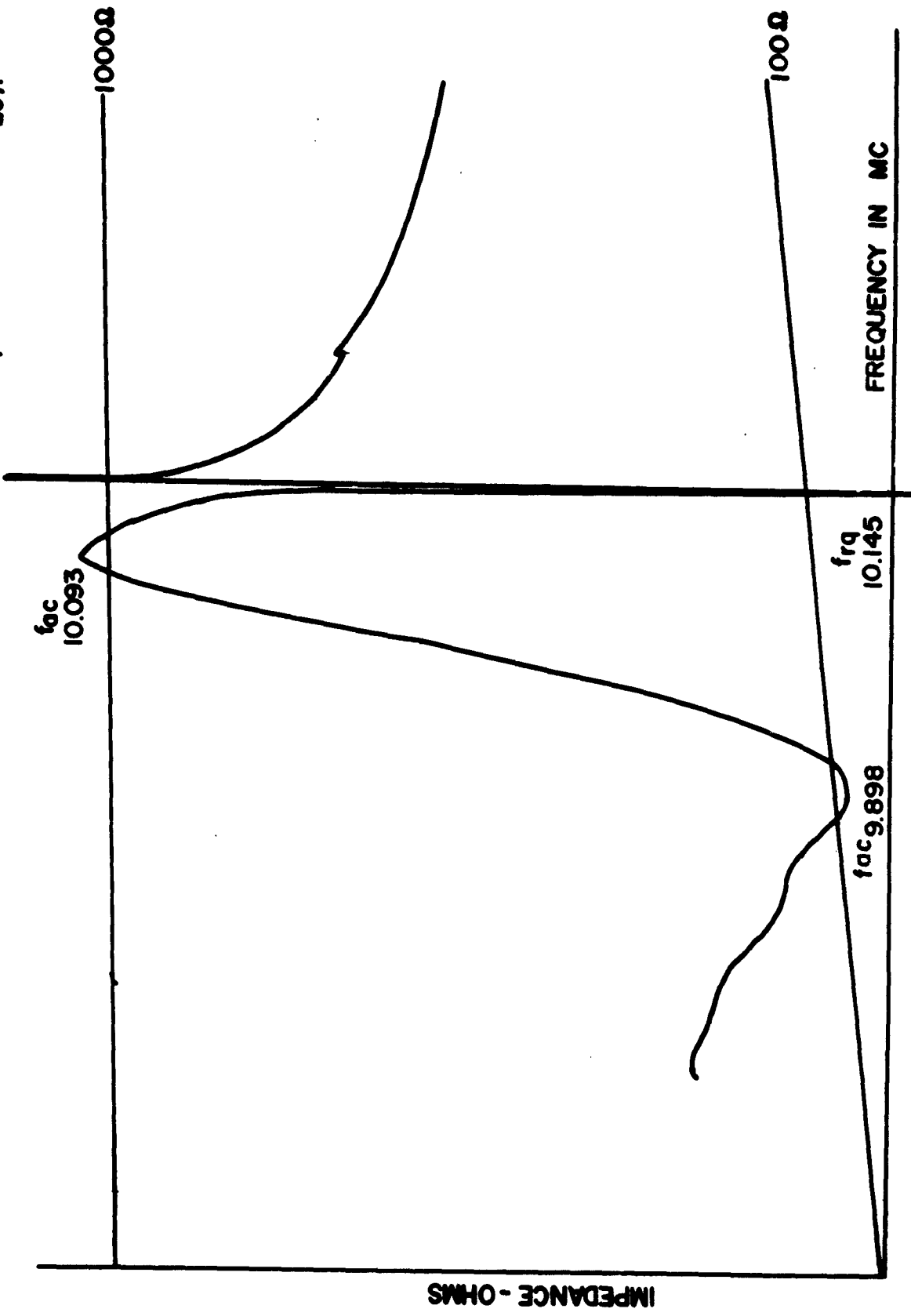
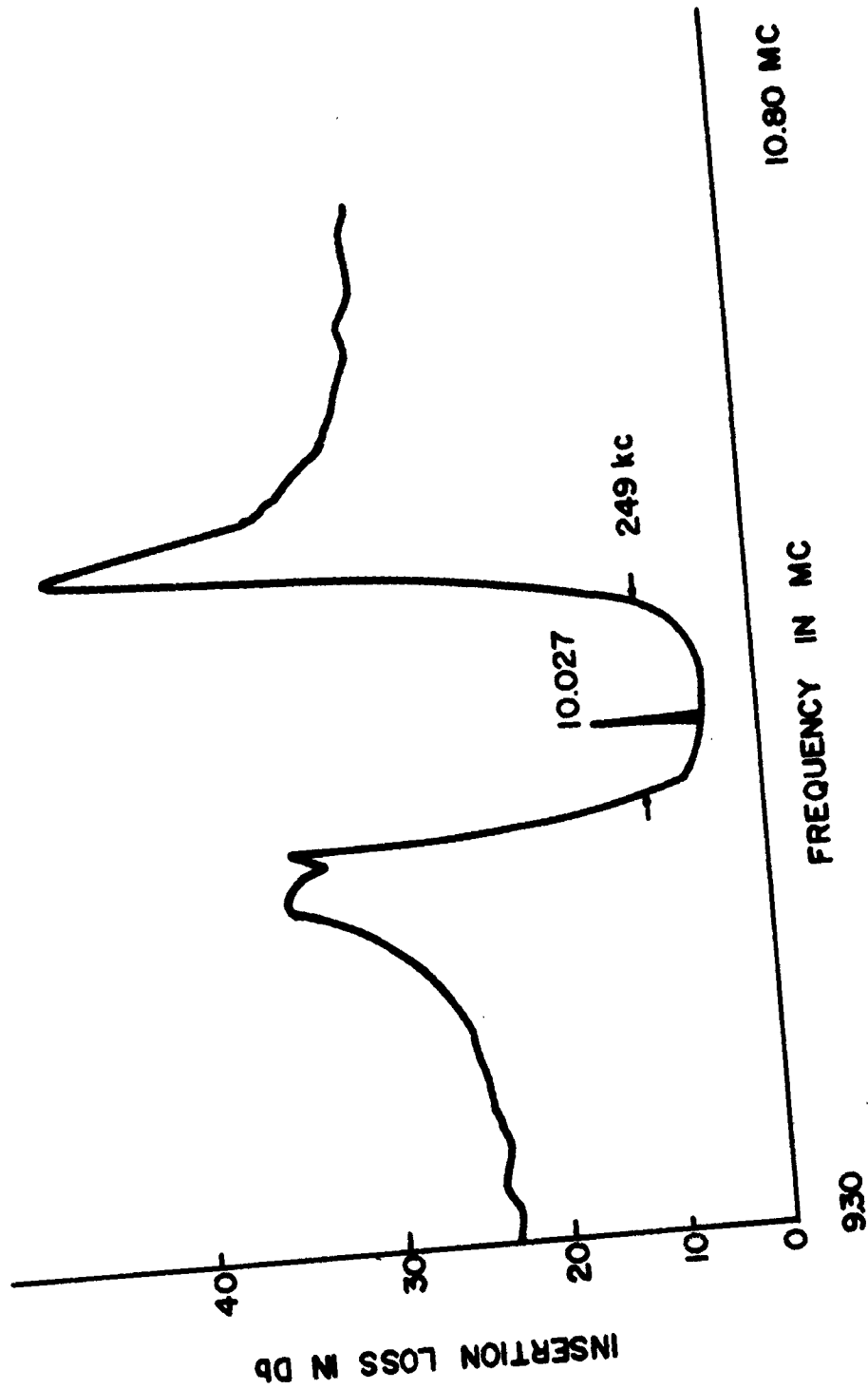


FIGURE 15. PARALLEL COMBINATION QUARTZ AND CERAMIC RESONATORS (f_{rq} GREATER THAN f_{ac}).



ERD 10454

FIGURE 16. SEVEN DOT-RESONATOR CERAMIC LADDER FILTER
WITH SINGLE PARALLEL QUARTZ RESONATOR.



ERD 10455

U. S. ARMY ELECTRONICS RESEARCH & DEVELOPMENT AGENCY
STANDARD DISTRIBUTION LIST
RESEARCH AND DEVELOPMENT CONTRACT REPORTS

	<u>Copies</u>
OASD (R&E) ATTN: Technical Library Room 3E1065 The Pentagon Washington 25, D. C.	1
Chief of Research and Development OCS, Department of the Army Washington 25, D. C.	1
Commanding General U. S. Army Materiel Command ATTN: R&D Directorate Washington 25, D. C.	1
Commanding General U. S. Army Electronics Command ATTN: AMSEL-AD Fort Monmouth, New Jersey	1
Director, U. S. Naval Research Laboratory ATTN: Code 2027 Washington 25, D. C.	1
Commander, Aeronautical Systems Division ATTN: ASAPRL Wright-Patterson Air Force Base, Ohio	1
Hq, Electronic Systems Division ATTN: ESAL L. G. Hanscom Field Bedford, Massachusetts	1
Commander, Air Force Cambridge Research Laboratories ATTN: CRO L. G. Hanscom Field Bedford, Massachusetts	1
Commander, Air Force Command & Control Development Division ATTN: CRZC L. G. Hanscom Field Bedford, Massachusetts	1

Copies

Commanding Officer
U. S. Army Electronics Research & Development Laboratory
ATTN: Technical Documents Center
Fort Monmouth, New Jersey

1

Commanding Officer
U. S. Army Electronics Research & Development Laboratory
ATTN: SELRA/ADJ (FU #1)
Fort Monmouth, New Jersey

1

Advisory Group on Electron Devices
346 Broadway
New York 13, New York

2

Commanding Officer
U. S. Army Electronics Research & Development Laboratory
ATTN: SELRA/TNR
Fort Monmouth, New Jersey
(FOR TRANSMITTAL TO ACCREDITED BRITISH AND
CANADIAN GOVERNMENT REPRESENTATIVES)

3

Commanding General
U. S. Army Combat Developments Command
ATTN: CDCMR-E
Fort Belvoir, Virginia

1

Commanding Officer
U. S. Army Combat Developments Command
Communications-Electronics Agency
Fort Huachuca, Arizona

1

Director, Fort Monmouth Office
U. S. Army Combat Developments Command
Communications-Electronics Agency
Building 410
Fort Monmouth, New Jersey

1

AFSC Scientific/Technical Liaison Office
U. S. Army Electronics Research & Development Laboratory
Fort Monmouth, New Jersey

1

Commanding Officer and Director
U. S. Navy Electronics Laboratory
San Diego 52, California

1

Copies

Chief, Bureau of Ships
Room 3327, Department of the Navy
ATTN: Mr. J. M. Kerr, Jr., (Code 691A2A)
Washington 25, D. C. 1

Commander, ARDC
ATTN: Mr. L. Grubbins, RACT
Griffiss Air Force Base, New York 1

General Electric Company
ATTN: Dr. S. Tehon
Electronics Park
Syracuse, New York 1

Illinois Institute of Technology
Electronics Research Laboratory
ATTN: Mr. E. Weber
3301 South Dearborn Street
Chicago 31, Illinois 1

Director
National Security Agency
Fort George C. Meade, Maryland
Attention: C3/TDL 1

Commander, ASD
ATTN: Mr. C. Green, ASRNE
Wright-Patterson Air Force Base, Ohio 1

Motorola, Inc.
ATTN: Mr. S. Malinowski
4545 W. Augusta Boulevard
Chicago 51, Illinois 1

Commanding Officer
U. S. A. Electronics Research & Development Laboratory
Fort Monmouth, New Jersey
ATTN: SELRA/PFP (Dr. Guttwein)
ATTN: SELRA/PEM (Mr. R. Sproat 1

USAELRDL Liaison Office
Rome Air Development Center
ATTN: RAOL
Griffiss Air Force Base, New York 1

Commanding Officer
U. S. A. Electronics Research & Development Laboratory
Fort Monmouth, New Jersey
ATTN: SELRA/PE (Dr. Both) 1
ATTN: SELRA/PE (Division Director) 1
ATTN: SELRA/PEM (Mr. N. Lipetz) 1

Copies